Exergoeconomic Analysis of a Pumped Heat Electricity Storage System with Concrete Thermal Energy Storage

Axel Dietrich[a], Frank Dammel[b], Peter Stephan[c]

[a,b,c] *Institute for Technical Thermodynamics, Technische Universität Darmstadt, Germany,*
[a] *dietrich@ttd.tu-darmstadt.de (CA)*
[b] *dammel@ttd.tu-darmstadt.de*
[c] *pstephan@ttd.tu-darmstadt.de*

[a,b,c] *Darmstadt Graduate School of Excellence Energy Science and Engineering,*
Technische Universität Darmstadt, Germany

Abstract:

Within the last 25 years the share of renewable energy sources in electrical energy production in Germany has been rising considerably. The volatility of renewable energy sources results in an increasing mismatch between supply and demand of electrical energy creating the need for storage capacities. The storage of electrical energy via the detour of thermal energy can be realized by a relatively new technology known as Pumped Heat Electricity Storage systems. This paper examines the exergoeconomic performance of such a storage system. A sample system comprising a concrete thermal energy storage is introduced; unsteady operations are simulated and analyzed. Although the achieved efficiencies are reasonable economical operations of the analyzed Pumped Heat Electricity Storage System are currently not possible. For the analyzed operation scenario the exergetic system efficiency, electrical energy output to electrical energy input, amounts to 27.3 %. Considering the storage capacity and the lack of geological requirements the Pumped Heat Electricity Storage system can compete with pumped hydrostorage and compressed air energy storage. However, prices of the order of 60 ct/(kWh) are not competitive considering current energy prices. Based on improved system designs as well as rising energy prices we assess Pumped Heat Electricity Storage Systems as a potential alternative to established storage technologies.

Keywords:
Pumped Heat Electricity Storage System, PHES, Concrete / Solid Media Thermal Energy Storage.

1. Introduction

Within the last 25 years the share of renewable energy sources in electrical energy production in Germany has been rising; amounting 23.40 % in 2013 (Fig. 1) [1]. Based on the trend shown in Fig. 1 we expect much higher shares of renewable energy sources in the future. The higher the share, the stronger is the impact of the volatility of renewable energy sources on the production of electrical energy. This results in a mismatch between the electrical energy supply and its demand at increasing intervals. To bridge supply and demand of electrical energy large scale storage systems are necessary. Chemical storage systems have limitations in capacity and lifetime and require relatively large amounts of rare elements which makes an application as large scale storage for electrical energy
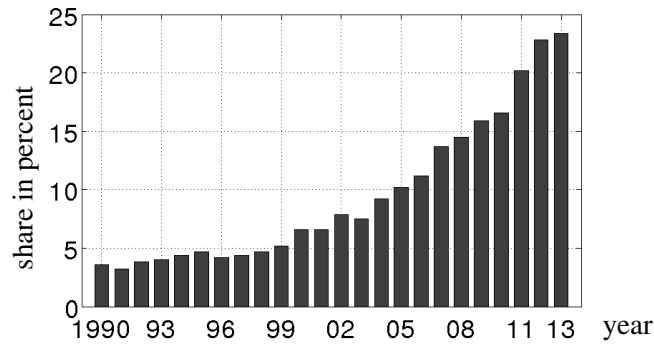
Fig. 1. Share of renewable energy sources in electrical energy production in Germany [1].

extremely difficult. Non-chemical storage systems such as pumped hydrostorage and compressed air energy storage can provide sufficient storage capacity but require special geological and geographical conditions [2] which limits their application as large scale storage for electrical energy. An alternative is the relatively new technology known as Pumped Heat Electricity Storage (PHES) systems which store electrical energy via the detour of thermal energy.

PHES systems consist of three to four subsystems (Fig. 2): a heat pump, one or two thermal energy storages, and a heat engine. In times of high supply and low demand the heat pump uses surplus electrical energy to pump heat taken from a low temperature thermal energy storage (or from the environment) to a higher temperature level. This high temperature heat is forwarded to the high temperature thermal energy storage, where it is stored until the demand for electrical energy exceeds its supply. At those times the thermal energy storage supplies heat to the heat engine which converts the thermal energy back into electrical energy. The low temperature heat released by the heat engine is absorbed by the low temperature thermal energy storage (or by the environment).

The few publications on PHES systems available in literature are based on different thermodynamic cycles as well as different types of thermal energy storage. Wolf [3] and Morandin et al. [4, 5] are using transcritical CO_2 Rankine cycles. The thermal energy is stored in one [3] or two [4, 5] pressurized water storages at temperatures between 155 °C and 175 °C. In addition, Morandin et al. use a saltwater-ice storage to store latent heat at −20 °C. The group around Desrue et al. [6] and Ruer et al. [7] is doing research on Brayton/Joule cycles with the working fluid argon in combination with two thermal energy storages operating at peak temperatures of 1000 °C and −70 °C. Howes [8] investigates a similar concept based on a Brayton/Joule cycle with two different working fluids air and argon. The thermal energy storage is composed of particulate minerals operating at peak temperatures of 500 °C and −160 °C. Thess [2] develops a thermodynamic model relating storage temperatures to overall storage system efficiency for certain boundary conditions.

The presented studies estimate the overall storage system efficiency, electrical energy output to electrical energy input, to amount to 60 % [4, 5] or 70 % and higher [6, 7, 8]. These estimations are slightly higher than the predictions made by [2].
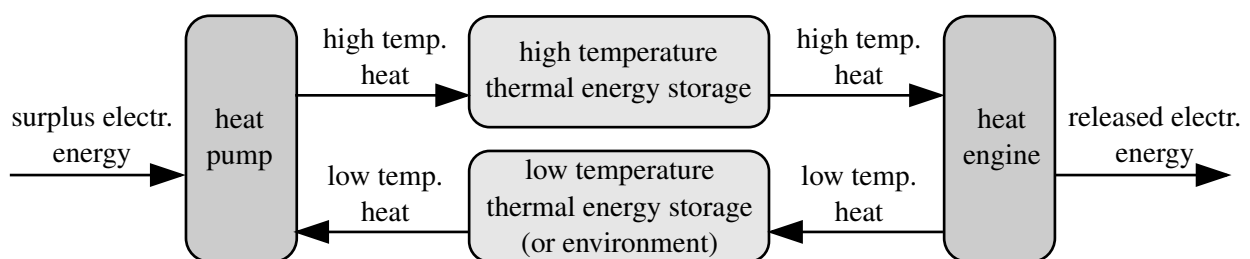

Fig. 2. General structure of a PHES system (boxes), including energy flows (arrows).

Besides efficiency estimates a detailed theoretical examination of the exergetic and economic performance of PHES systems has not been carried out so far. Therefore we examine the exergoeconomic performance of a PHES system in order to answer the question whether such storage systems can be operated reasonably from an exergetical and economical point of view.

2. Methodology

In this section we first describe the design and model of the PHES system. Second, the analyses methods are presented, starting with the exergy analysis, followed by the economic analysis and completed with the exergoeconomic analysis.

2.1. Design and model of the PHES system

During the design of the PHES system and the selection of the components the focus was set on employing as much established technology as possible. Therefore, the PHES system consists of a vapor compression heat pump and an Organic Rankine Cycle (ORC), both running with the working fluid butane (C_4H_{10}). As high temperature storage a sensible solid media thermal energy storage with high temperature concrete is selected. For the low temperature thermal energy storage the environment is taken as heat reservoir (Fig. 2).

For most technical systems the exergetic and economic efficiencies increase with increasing system size. However, the larger the PHES system, the larger will be the technological risks and uncertainties. As a compromise we chose a medium-sized PHES system, having an electrical energy output per discharge cycle of $En_{el,out} = 320\,kWh$.

The system is modeled in the process simulation software EBSILON®*Professional*. All components of the heat pump and heat engine are simulated quasi-stationarily. The thermal energy storage is simulated unsteadily by a finite differences Crank–Nicolson method.

2.1.1. Heat pump and heat engine

The Carnot efficiency of heat pumps decreases with increasing maximum cycle temperature whereas the Carnot efficiency of heat engines increases with increasing maximum cycle temperature. For thermodynamically ideal cycles the product of heat pump and heat engine efficiency is equal to one, independent of the maximum cycle temperature. For real systems the product is less than one and depends, among other parameters, on the maximum cycle temperature. In a preliminary study we examined the effect of maximum cycle temperature and working fluid on the product of vapor compression heat pump and ORC heat engine efficiency. As a result we suggest an average storage temperature of 135 °C in combination with the working fluid butane.

Currently available heat pumps do not deliver maximum cycle temperatures above 100 °C. Therefore the heat pump design results from a combination of individual components (Fig. 3). The selection of design point temperatures and pressures (Fig. 4, Table 1) is based on the availability of suitable components. However, compressors providing both, appropriate volume flows and compression ratios, could not be identified. Consequently, a series of four compressors having a suitable power in combination with an appropriate compression ratio is selected.

ORCs operating with maximum cycle temperatures in the range of 135 °C are state of the art. Suitable components are available (Fig. 3), and appropriate design point temperatures and pressures are selected (Fig. 4, Table 1). The design point performance of the PHES system is given in Table 2.
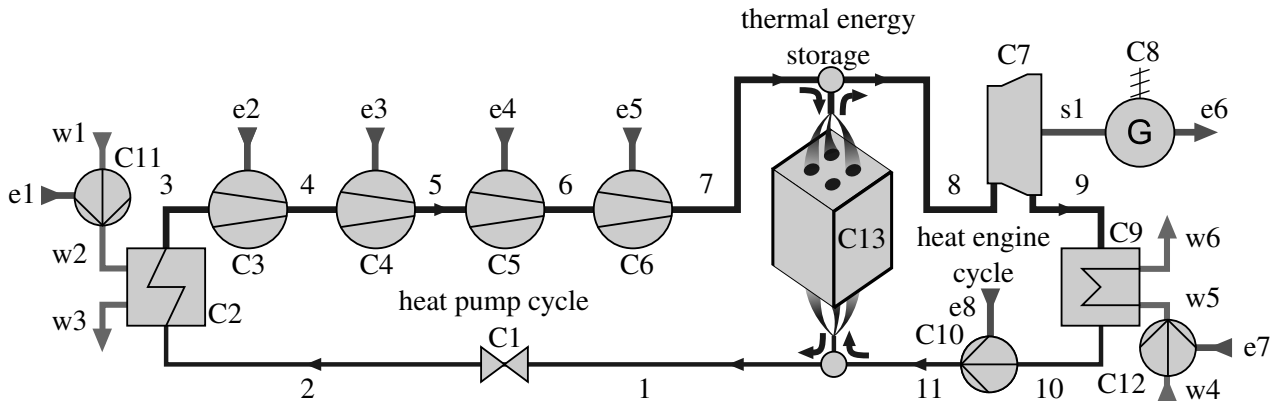
Fig. 3. Labeled model of the PHES system. Thin lines without prefix: butane lines (liquid); thick lines without prefix: butane lines (vapor); prefix w: water lines; prefix e: electric lines; prefix s: shaft; prefix C: components.
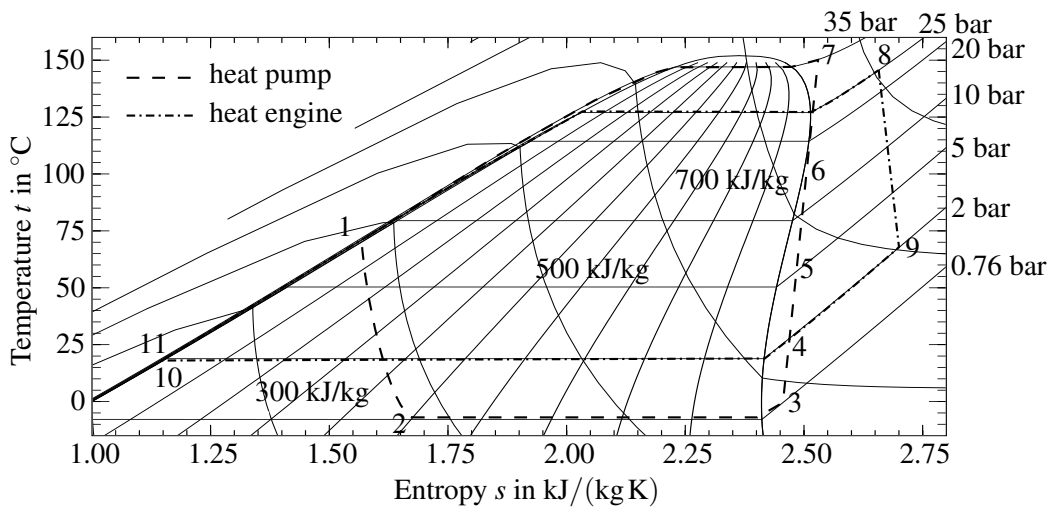

Fig. 4. Labeled t,s-diagram of the PHES system using butane as working fluid. Source of plain diagram: [9].

Table 1. Design point states of the PHES system. The line numbers refer to the labels in Fig. 3.

line	1	2	3	4	5	6	7	8	9
t in °C	70.0	−6.6	−3.8	28.0	60.0	97.4	150.5	145.2	67.1
p in bar	34.9	0.80	0.76	1.9	5.0	13.3	35.0	25.0	2.00
h in kJ/kg	376.4	376.4	586.8	628.9	676.0	723.8	764.6	803.0	700.8
X in %	0	49.0	100	100	100	100	100	100	100

line	10	11	w1	w2	w3	w4	w5	w6
t in °C	17.3	18.6	10.0	10.0	4.0	10.0	10.0	13.8
p in bar	1.9	25.1	1.01	1.70	1.20	1.01	1.70	1.20
h in kJ/kg	240.7	245.7	42.12	42.20	16.93	42.12	42.20	58.25
X in %	0	0	0	0	0	0	0	0

Table 2. Performance data of the PHES system at the design point.

	$\dot{M}_{C_4H_{10}}$ in kg/s	$\dot{M}_{H_2O}$ in kg/s	$\dot{Q}_{in}$ in kW	$\dot{Q}_{out}$ in kW	P_{in} in kW	P_{out} in kW
Heat pump	0.860	7.16	181.0	333.9	165	-
Heat engine	0.869	24.9	484.3	399.8	7.0	87.4

2.1.2. Thermal energy storage

Based on a prototype and studies by the *German Aerospace Center (DLR)* [10, 11, 12] we select a sensible solid media thermal energy storage built of high temperature concrete. The concrete is traversed by heat exchanger tubes transmitting the working fluid. Mass M and volume V (Fig. 5) of the storage medium are calculated based on the amount of electrical energy output per discharging period $En_{el,out}$ as defined in section 2.1. For a given mass flow, the cross sectional area of the heat exchanger tubes and the amount of tubes defines the fluid velocity inside the tubes. To enhance heat transfer to/from the fluid the tube diameter and the amount of tubes are chosen to always result in Reynolds numbers $Re \geq 10^4$, which guaranties turbulent flow conditions. The tube distance a, adapted from [12], in combination with the amount of tubes and the storage volume V define the outer dimensions of the storage (Fig. 5). Physical properties of the storage material are taken from the studies by the *German Aerospace Center* [10, 11, 12].

When passing through the heat exchanger tubes inside the storage the working fluid experiences a phase change vapor→liquid (charging period) or liquid→vapor (discharging period). Due to the phase change the convective heat transfer coefficient α between working fluid and heat exchanger tubes varies with the flow characteristics and cannot be calculated exactly by solely analytical means. For fully developed turbulent pipe flow [13] the convective heat transfer coefficient is estimated conservatively by considering the entirely liquid fluid only. The same simplification and the conservative assumption of heavily fouled tubes is applied to approximate the working fluid pressure drop inside the heat exchanger tubes [14].

For a lean numerical simulation, instead of the entire storage (Fig. 5), a single cylindrical storage segment (Fig. 6) is modeled. As the storage segments do not cover the entire storage volume (Fig. 6) the outer diameter of each single storage segment a^* is increased compared to the tube distance a. By selecting a ratio of $a^*/a = 1.050$ the total storage mass of all cylindrical storage segments is
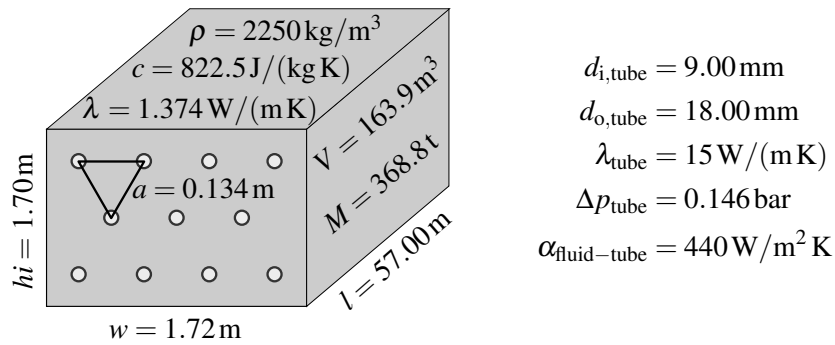

Properties shown in figure:
$\rho = 2250\,\text{kg/m}^3$
$c = 822.5\,\text{J/(kg K)}$
$\lambda = 1.374\,\text{W/(m K)}$
$V = 163.9\,\text{m}^3$
$M = 368.8\,\text{t}$
$a = 0.134\,\text{m}$
$hi = 1.70\,\text{m}$
$l = 57.00\,\text{m}$
$w = 1.72\,\text{m}$

$d_{i,\text{tube}} = 9.00\,\text{mm}$
$d_{o,\text{tube}} = 18.00\,\text{mm}$
$\lambda_{\text{tube}} = 15\,\text{W/(m K)}$
$\Delta p_{\text{tube}} = 0.146\,\text{bar}$
$\alpha_{\text{fluid}-\text{tube}} = 440\,\text{W/m}^2\,\text{K}$

Fig. 5. *Structure and properties of the solid media thermal energy storage. For simplicity the illustration does only show 12 heat exchanger tubes. The real setup contains a total of 188 tubes assembled in 15 rows of 13 and 12 tubes (alternating).*
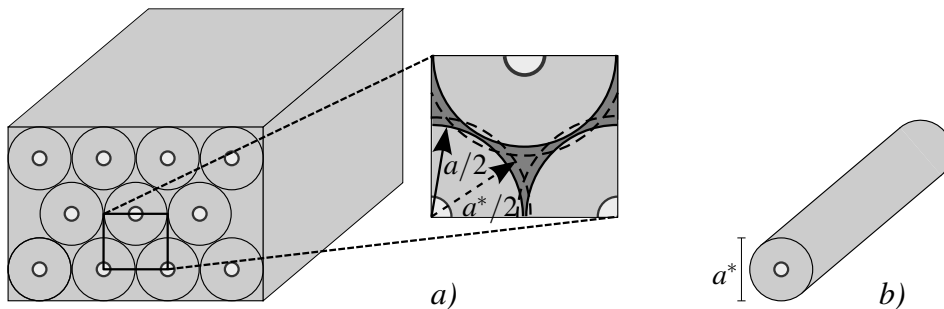

Fig. 6. *a) Segmentation of the solid media thermal energy storage into cylinders; b) modeled single cylindrical storage segment.*

equal to the mass of the rectangular shaped storage. The model does not consider any heat losses to the environment.

2.2. Exergy analysis

If a system of an arbitrary state S is brought reversibly into equilibrium with the environment the work done by the system during this process is equal to the system exergy in state S. Consequently, exergies quantify the maximum amount of work a system of a specific state could release in a specific environment. Exergy balances of energy conversion processes show exergy destructions which indicate the degree of process irreversibility and thereby evaluate the quality of energy conversion. An exergy analysis of the PHES system is conducted to evaluate its performance on system, subsystem and component level.

The specific exergy of the butane and water flows of an arbitrary state S is calculated according to

$$e_{\mathrm{S}} = h_{\mathrm{S}} - h_{\mathrm{ref}} - T_{\mathrm{ref}} \left(s_{\mathrm{S}} - s_{\mathrm{ref}} \right). \qquad (1)$$

For both fluids, the reference temperature is set to the ambient temperature $T_{\mathrm{ref,butane}} = T_{\mathrm{ref,water}} = 283.15\,\mathrm{K}$. To determine the reference entropy s_{ref} the reference pressure p_{ref} needs to be defined. As liquid water is existent under ambient conditions, its reference pressure is set equal to the ambient pressure $p_{\mathrm{ref,water}} = 1.01\,\mathrm{bar}$. Butane does not exist in the atmospheric environment to a measurable extent. Consequently, butane leaving the PHES system expands to a vanishing partial pressure, which defines its reference pressure $p_{\mathrm{ref,butane}} = 0\,\mathrm{bar}$.

Charging (heat pump operation) or discharging (heat engine operation) of the PHES system results in a changing temperature distribution inside the solid media thermal energy storage. Therefore the temperature of the working fluid leaving the storage is varying, too. The working fluid is fed back into the cycle and influences the heat pump or heat engine operation (depending on the current operation mode). Consequently, the operation of the PHES system is time-dependent and cannot be analyzed by a steady-state approach.

The time-dependent exergy analysis is based on the total amount of exergy entering and leaving each individual component during a complete charging, storage and discharging period. The total amount of exergy entering and leaving each component is determined by integrating the exergy flow that passes through the lines attached to each component (Fig. 3) over a complete operation period. To produce representative results the integration has to be done over a representative operation period.

To determine a representative operation period several consecutive charging, storage and discharging periods are simulated. Once the total amount of exergy passing through each individual line in the cycle is constant from period to period, the representative operation period is found. All representative operation periods have the following characteristics:

- same temperature distribution inside the thermal energy storage at corresponding times,
- same total amount of exergy entering and leaving a particular component,
- all charging and discharging periods take the same time.

The results presented in Section 3 are based on the analysis of a representative operation period. The exergy destruction within a component C is calculated by the exergy balance

$$E_{\mathrm{D,C}} = \sum E_{\mathrm{in,C}} - \sum E_{\mathrm{out,C}}. \qquad (2)$$

Based on the component specific definitions of product $E_{\mathrm{P,C}}$ and fuel exergies $E_{\mathrm{F,C}}$, which are presented next to the results in Table 7, the exergy efficiency of a component C is defined by

$$\eta_{\mathrm{ex,C}} = \frac{E_{\mathrm{P,C}}}{E_{\mathrm{F,C}}}. \qquad (3)$$

2.3. Economic analysis

We conduct an economic analysis of the PHES system to assign costs to each component of the system. First, the purchased equipment costs are determined for each component. Second, levelized annual costs are calculated, considering purchased equipment costs as well as operation and maintenance costs. Finally, the component costs per operation period are calculated, which are necessary for the exergoeconomic analysis.

Purchased equipment costs based on actual market prices could not be identified for all components of the PHES system. For consistency the purchased equipment costs of all components except the generator and the solid media thermal energy storage are determined using the module factor approach in the form presented by Turton et al. [15]. Based on a survey of equipment manufacturers the purchased equipment costs Z_C^{PEC} of a component C are fitted to the equation

$$Z_C^{PEC} = e3K_{C,1} + K_{C,2}\log_{10}A_C + K_{C,3}(\log_{10}A_C)^2,$$
(4)

with A_C being the capacity/size parameter and $K_{C,1}\ldots K_{C,3}$ being the fitting parameters of component C, respectively. We take fitting and capacity/size parameters from Turton et al. [15] to calculate the purchased equipment costs (Table 3).

The purchased equipment cost of the generator and the solid media thermal energy storage (Table 3) are determined applying the six-tenth rule, as described in [15],

$$Z_C^{PEC} = Z_{ref}^{PEC}\left(\frac{A_C}{A_{ref}}\right)^{0.6}.$$
(5)

Reference costs Z_{ref}^{PEC} and reference capacity/size parameters A_{ref} are taken from [17] (generator) and [18] (solid media thermal energy storage).

Costs in US-Dollar are converted to Euro applying an exchange rate of $1 \text{€} = 1.14\text{\$}$. The purchased equipment costs of the throttle valve (C1) are negligible compared to all other components and there-

Table 3. *Calculation parameters A, K_1, K_2, K_3, purchased equipment costs Z^{PEC}, annual investment costs Z^{an} and investment costs per operation period Z for all PHES components.*

Component (Figure 3)	A_C	$K_{C,1}$	$K_{C,2}$	$K_{C,3}$	Z^{PEC} in 10^3 €	Z^{an} in 10^3 €	Z in €
C1					0	0	0
C2	95.2 m² [1]	4.6656	−0.1557	0.1547	80.59	10.04	27.5
C3	41.0 kW	5.0355	−1.8002	0.8253	16.67	2.076	5.69
C4	41.0 kW	5.0355	−1.8002	0.8253	16.67	2.076	5.69
C5	41.0 kW	5.0355	−1.8002	0.8253	16.67	2.076	5.69
C6	41.0 kW	5.0355	−1.8002	0.8253	16.67	2.076	5.69
C7	100 kW	2.7051	1.4398	−0.1776	65.67	8.180	22.4
C9	356 m² [1]	4.6656	−0.1557	0.1547	165.5	20.61	56.5
C10	4.41 kW	3.3892	0.0536	0.1538	2.696	0.336	0.92
C11	1.00 kW	3.3892	0.0536	0.1538	2.149	0.268	0.73
C12	2.19 kW	3.3892	0.0536	0.1538	2.336	0.291	0.79
C8	$A = 88.7\,\text{kW}, A_{ref} = 15945\,\text{kW}, Z_{ref}^{PEC} = 800 \cdot 10^3\,\text{\$}$				31.13	3.878	10.6
C13	$A = 369\,\text{t}, A_{ref} = 42.7\,\text{t}, Z_{ref}^{PEC} = 9120\,\text{€}$				33.25	4.142	11.3
Σ					450.0	56.04	153.5

[1] Based on a conservatively selected overall heat transfer coefficient $k = 185\,\text{W}/(\text{m}^2\text{K})$ for plate heat exchangers [16].

Table 4. Durations of the PHES operation periods within the characteristic operation scenario. Due to a 24h simulation of the PHES system, storage period II bridges the time between a discharging and charging period.

Charging period	Storage period I	Discharging period	Storage period II
7 h	1 h	4 h	12 h

fore have been set to zero.

The capital recovery factor, as described in [19], is used to levelize the purchased equipment costs over the entire projected PHES operation period of $n = 20$ years taking compounded interest at an interest rate of $ir = 9\%$ into account. In addition, a constant factor $\gamma = 0.015$ year^{-1} is introduced to estimate the annual operation and maintenance costs [19]. Consequently, the annual investment costs become

$$Z_C^{an} = \left(\frac{ir(1+ir)^n}{(1+ir)^n - 1} + \gamma \right) Z_C^{PEC}. \qquad (6)$$

To calculate the investment costs per operation period, we determine the amount of operation periods per year. Based on the development of electricity prices in the day-ahead auction for Germany at the European Power Exchange (EPEX SPOT) [20] we define four characteristic operation scenarios for each season of the year. Independent of the season each day has a period of approximately 7 hours of low electricity prices (roughly between 23 and 6h) and a period of approximately 4 hours of high electricity prices (roughly between 7 and 11h). Therefore, a characteristic operation scenario is based on a single charging, storage, and discharging period per day/24 hours (Table 4). Finally, the investment costs per operation period can be determined (Table 3).

Based on the characteristic operation scenario and data provided by [20] the specific costs for electrical energy entering the heat pump are determined to $c_{el} = 2.43$ ct/(kWh). Assuming an access to a natural water source, the specific costs for water entering and exiting the PHES system are defined to $c_{H_2O} = 0$.

2.4. Exergoeconomic analysis

An exergoeconomic analysis combines exergy and economic analysis by assigning costs to exergies. We use the method by Tsatsaronis [21, 19] that relates the costs C_S to the exergy E_S using

$$C_S = c_S \cdot E_S. \qquad (7)$$

The specific costs per exergy c_S are determined for each state S in the cycle by solving the linear system of equations resulting from a cost balances around each component C:

$$\sum C_{in,C} + Z_C = \sum C_{out,C}$$
$$\sum (c_{in,C} \cdot E_{in,C}) + Z_C = \sum (c_{out,C} \cdot E_{out,C}). \qquad (8)$$

To solve the linear system auxiliary equations are defined for each component (Table 5) that has

- an inflow crossing the system boundary (incoming water or incoming electrical energy),
- more than one outflow.

3. Results

All results presented in this section refer to the energetic and exergetic analysis of a representative operation period, as defined in Section 2.2.

Table 5. Auxiliary equations necessary to solve the linear system of equations (8).

Component	Auxiliary equation	Description
C3, C4, C5, C6, C11	$c_{ei} = c_{el}$ $i \in [1-5]$	With the electrical energy entering the compressors and the pump specific costs enter the heat pump subsystem.
C10, C12	$c_{e7} = c_{e8} = c_{e6}$	The electrical energy consumed by the pumps of the heat engine is supplied by the generator (C8).
C11, C12	$c_{w1} = 0$ $c_{w4} = 0$	The water entering the pumps is supplied by a natural source and therefore has no costs assigned.
C2, C9	$c_{w3} = 0$ $c_{w6} = 0$	The water leaving the evaporator and the condenser has no further use and therefore has no costs assigned.
C13	$c_1 = 0$	All costs exiting the storage are assigned to line 8.
C7	$c_9 = 0$	All costs exiting the turbine are assigned to line s1.

The development of storage temperatures and cycle efficiencies is depicted in Fig. 7. During heat pump operation the mean temperature of the thermal energy storage and the storage outlet temperature of the working fluid increases. This results in a decrease of heat absorbed by the thermal energy storage with increasing heat pump operation time. Consequently, the energetic and exergetic efficiencies decrease with increasing heat pump operation time. During heat engine operation the mean temperature of the thermal energy storage and the storage outlet temperature of the working fluid decreases. With increasing heat engine operation time, the heat provided by the thermal energy storage as well as the electrical energy produced by the generator decrease proportionally resulting in a constant energetic efficiency. As the maximum cycle temperature decreases with increasing heat engine operation time, the exergetic efficiency increases slightly.

The exergy flows passing trough all lines of the PHES system integrated individually over the characteristic operation period are listed in Table 6. These values are the basis of all following results.

The exergy destruction E_D in the thermal energy storage and the heat engine are approximately equal, whereas the heat pump produces an exergy destruction which is almost 5 times higher (Table 7). The exergetic efficiencies show the same trend. The heat pump performs worst, while thermal energy storage and heat engine operate roughly in the same range. The throttle valve and the cascaded compressors are the main reason for the low heat pump performance, destroying a total of $E_{D,\text{th.+comp.}} = (320 + 215)\text{kWh} = 535\,\text{kWh}$ of exergy per charging period.

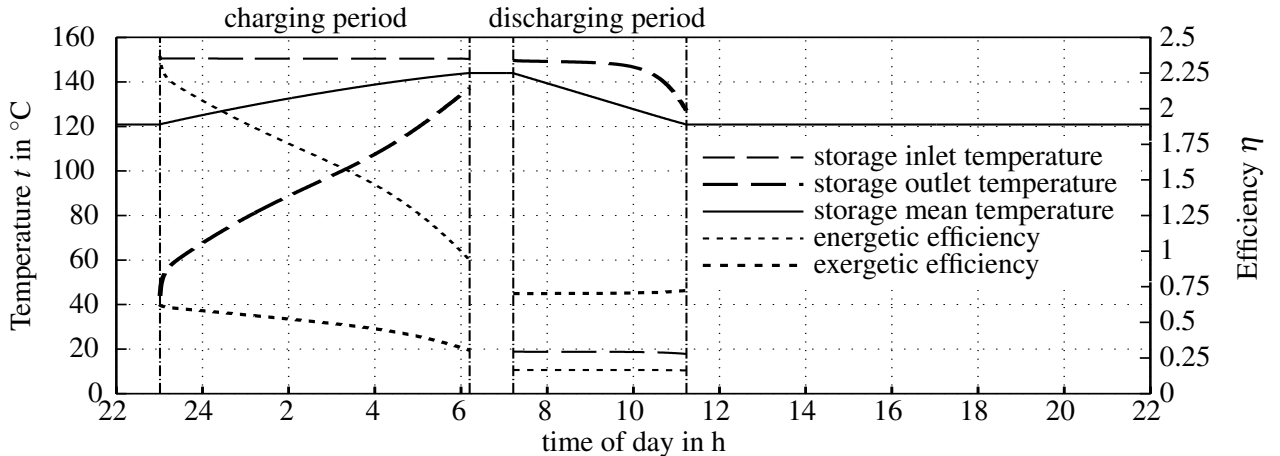The current model does not consider heat losses to the environment. Therefore the energetic efficiency

Fig. 7. Storage temperatures and process efficiencies over operation time. Heat pump operation: 23 - 6 h, heat engine operation: 7 - 11 h.

Table 6. Integrated exergy amounts at each line of the PHES system.

line	1	2	3	4	5	6	7	8	9
E in kWh	7258	6938	6873	7097	7352	7614	7842	4446	4046
line	10	11	w1	w2	w3	w4	w5	w6	s1
E in kWh	3972	3987	0	2.3	10.6	0	6.7	12.9	358.5
line	e1	e2	e3	e4	e5	e6	e7	e8	
E in kWh	3.7	280.5	313.5	318.6	271.7	352.9	9.4	18.9	

Table 7. Product E_P and fuel exergy E_F definitions, exergy destruction E_D, as well as energetic η_{en} and exergetic η_{ex} efficiencies of all components, the subsystems, and the PHES system.

Component	E_P	E_F	E_D in kWh	η_{en} in %[2]	η_{ex} in %
C1	E_2	E_1	320	100	95.6
C2	E_3	$E_2 + E_{w2} - E_{w3}$	57.0	100	99.2
C3	$E_4 - E_3$	E_{e2}	56.3	93.1	79.9
C4	$E_5 - E_4$	E_{e3}	58.9	93.1	81.2
C5	$E_6 - E_5$	E_{e4}	56.0	93.1	82.4
C6	$E_7 - E_6$	E_{e5}	44.0	93.1	83.8
C7	E_{s1}	$E_8 - E_9$	41.9	99.8	89.5
C8	E_{e6}	E_{s1}	5.63	98.4	98.4
C9	E_{10}	$E_9 + E_{w5} - E_{w6}$	67.4	100	98.3
C10	$E_{11} - E_{10}$	E_{e8}	4.88	92.1	74.2
C11	$E_{w2} - E_{w1}$	E_{e1}	1.34	90.0	63.7
C12	$E_{w5} - E_{w4}$	E_{e7}	2.48	92.1	73.7
heat pump	$E_7 - E_1$	$E_{e1} + E_{e2} + E_{e3} + E_{e4} + E_{e5}$	593	165	49.2
th. en. storage	$E_8 - E_{11}$	$E_7 - E_1$	125	100	78.7
heat engine	$E_{e6} - E_{e7} - E_{e8}$	$E_8 - E_{11}$	122	16.6	70.6
PHES system	$E_{e6} - E_{e7} - E_{e8}$	$E_{e1} + E_{e2} + E_{e3} + E_{e4} + E_{e5}$	840	27.3	27.3

[2] Energetic efficiencies are based on energetic product and fuel definitions equivalent to the exergetic definitions given in this table.

Table 8. Exergy E, specific costs per exergy c and costs C entering and leaving the PHES subsystems per operation period (24 hours).

	Electricity to heat pump	Heat to th. en. storage	Heat from th. en. storage	Heat engine net electricity output
E in kWh	1188	584.2	459.7	324.5
c in ct/(kWh)	2.43	13.67	19.84	56.21
C in €	28.87	79.85	91.20	182.42

of throttle valve, evaporator, condenser, and thermal energy storage amounts to 100%.

On its course through the PHES system the exergy entering and leaving each subsystem decreases, whereas the costs increase (Table 8). The solid media thermal energy storage causes the smallest increase in absolute and specific costs, followed by the heat pump and the heat engine subsystem.

4. Discussion and Conclusions

For this relatively simple PHES system with moderate storage temperatures the overall system efficiency amounts to $\eta_{ex} = \eta_{en} = 27.3\%$, which is considerable. Although exergetic efficiencies of

pumped hydrostorage and compressed air energy storage systems can be more than twice as high, PHES systems have the advantage of providing huge storage capacities without being bound to geological requirements. In contrast, the formerly mentioned storage technologies are bound to geological requirements. However, the economic performance of the analyzed PHES system is rather weak. The calculated prices for the released electrical energy are not competitive considering current energy prices. Nevertheless, further research on PHES systems should be conducted, as system improvements, an onward increasing share of renewable energy sources in electrical energy production, and rising prices for fossil fuels are to expect.

We developed a model of a specific PHES system in combination with a calculation procedure considering characteristic operation scenarios. Model and calculation procedure can be modified with reasonable effort to analyze different configurations. However, the model lacks the quantification of uncertainties, which are especially important with respect to the estimation of costs. In addition, heat losses to the environment are not considered yet. Therefore, the analysis method will be improved to account for uncertainties and heat losses. For further studies, different types of thermodynamic cycles and different types of thermal energy storage will be modeled.

Acknowledgements

Nomenclature

Latin symbos

a	tube distance, m
A	capacity or size parameter
c	specific heat capacity, J/(kg K)
d	diameter, mm
E	exergy, kWh
En	energy, kWh
h	enthalpy, kJ/kg
hi	height, m
ir	interest rate, %
K	constant
l	length, m
M	mass, t
n	projected operation period, a
p	pressure, bar
s	entropy, kJ/(kg K)
t	temperature, °C
V	volume, m^3
w	width, m
X	steam quality, %

Greek symbos

α	convective heat transfer coefficient, W/(m^2 K)
η	efficiency, %
γ	annual operation and maintenance costs factor
λ	heat conductivity, W/(m K)
ρ	density, kg/m^3

Superscripts, Subscripts and Abbreviations

an	annual
C	component
D	destruction
F	fuel
i	inner
in	inflow
o	outer
ORC	Oragnic Rankine Cycle
out	outflow
P	product
PEC	purchased equipment cost
PHES	pumped heat electricity storage
S	state

References

[1] AG Energiebilanzen. Share of renewable energy sources in electrical energy production in germany from 1990 to 2013. Technical report, Germany, 2014.

[2] A. Thess. Thermodynamic efficiency of pumped heat electricity storage. *Physical Review Letters*, 111(11):110602, 2013.

[3] B. Wolf. Method for storing and recovering energy. Patent No.: EP 1987299 b1, January 2007.

[4] M. Morandin, F. Maréchal, M. Mercangöz, and F. Buchter. Conceptual design of a thermo-electrical energy storage system based on heat integration of thermodynamic cycles – part a: Methodology and base case. *Energy*, 45(1):375–385, 2012.

[5] M. Morandin, F. Maréchal, M. Mercangöz, and F. Buchter. Conceptual design of a thermo-electrical energy storage system based on heat integration of thermodynamic cycles – part b: Alternative system configurations. *Energy*, 45(1):386–396, 2012.

[6] T. Desrues, J. Ruer, P. Marty, and J. Fourmigué. A thermal energy storage process for large scale electric applications. *Applied Thermal Engineering*, 30(5):425–432, 2010.

[7] J. Ruer, E. Sibaud, T. Desrues, and P. Muguerra. Pumped heat energy storage. Technical report, Saipem, France, 2010.

[8] J. Howes. Concept and development of a pumped heat electricity storage device. *Proceedings of the IEEE*, 100(2):493–503, 2012.

[9] REFPROP. NIST standard reference database 23. Version 9.0, 2010.

[10] D. Laing, D. Lehmann, and C. Bahl. Concrete storage for solar thermal power plants and industrial process heat. In *Proceedings of the Third International Renewable Energy Storage Conference (IRES 2008)*, Berlin, November 2008.

[11] D. Laing, D. Lehmann, M. Fiß, and C. Bahl. Test results of concrete thermal energy storage for parabolic trough power plants. *J. Sol. Energ. Engin.*, 131(4):041007–041007, September 2009.

[12] D. Laing, C. Bahl, T. Bauer, M. Fiss, N. Breidenbach, and M. Hempel. High-temperature solid-media thermal energy storage for solar thermal power plants. *Proceedings of the IEEE*, 100(2):516–524, February 2012.

[13] V. Gnielinski. G1 heat transfer in pipe flow. In VDI-GVC, editor, *VDI Heat Atlas*, pages 691–700. Springer, Berlin, Heidelberg, 2010.

[14] W. Kast, H. Nirschl, E. S. Gaddis, K.-E. Wirth, and J. Stichlmair. L1 pressure drop in single phase flow. In VDI-GVC, editor, *VDI Heat Atlas*, pages 1053–1116. Springer, Berlin, 2010.

[15] R. Turton, R. C. Bailie, W. B. Whiting, J. A. Shaeiwitz, and D. Bhattacharyya. *Analysis, synthesis, and design of chemical processes*. Pearson, Upper Saddle River, 4th edition, 2013.

[16] W. Roetzel and B. Spang. C3 typical values of overall heat transfer coefficients. In VDI-GVC, editor, *VDI Heat Atlas*, pages 75–78. Springer, Berlin, Heidelberg, 2010.

[17] O. Balli, H. Aras, and A. Hepbasli. Exergoeconomic analysis of a combined heat and power (CHP) system. *International Journal of Energy Research*, 32(4):273–289, 2008.

[18] D. Laing, W. D. Steinmann, P. Viebahn, F. Gräter, and C. Bahl. Economic analysis and life cycle assessment of concrete thermal energy storage for parabolic trough power plants. *Journal of Solar Energy Engineering*, 132(4):041013–041013, October 2010.

[19] A. Bejan, G. Tsatsaronis, and M. Moran. *Thermal Design and Optimization*. Wiley, 1995.

[20] EPEX SPOT - European Power Exchange. Market data day-ahead auction. Website, http://www.epexspot.com/en/market-data/dayaheadauction, February 2015.

[21] G. Tsatsaronis. Thermoeconomic analysis and optimization of energy systems. *Progress in Energy and Combustion Science*, 19(3):227–257, 1993.